

# Scanning Electron Microscopy Study of Raw and Chemically Modified Sisal Fibers

Maria Alice Martins,<sup>1</sup> Pedro Kunihiro Kiyohara,<sup>2</sup> Inés Joeques<sup>3</sup>

<sup>1</sup>Embrapa Instrumentação Agropecuária, CP 741, 13560-970, São Carlos, Brazil

<sup>2</sup>Laboratório de Microscopia Eletrônica, Instituto de Física, Universidade de São Paulo, CP 66318, 05315-970, São Paulo, Brazil

<sup>3</sup>Instituto de Química, Universidade Estadual de Campinas, CP 6154, 13083-970, Campinas, Brazil

Received 20 October 2003; accepted 27 July 2004

DOI 10.1002/app.21203

Published online 22 October 2004 in Wiley InterScience (www.interscience.wiley.com).

**ABSTRACT:** Mercerization and acetylation treatments were applied to sisal fibers to enhance adhesion with polymer matrices in composites. The structures of the untreated and treated fibers were assessed with scanning electron microscopy. The waste from sisal-fiber decortication consisted of mechanical, ribbon, and xylem fibers, and their ultimate cells varied considerably in size and shape. After mercerization and acetylation, the fibers and conductive-vessel surfaces were successfully changed. The parenchyma cells were partially removed, and the fibrils started to split,

because of the alkali action. This increased the effective surface area available for contact with the matrix. The mercerized and acetylated fibers were coated with cellulose acetate by the grafting of the acetyl group in the fibrils. The treatment used to remove lignin and hemicellulose caused changes in the fiber surface but did not damage the fiber structure because the fibrils remained joined in a bundle. © 2004 Wiley Periodicals, Inc. *J Appl Polym Sci* 94: 2333–2340, 2004

**Key words:** fibers; morphology; microstructure

## INTRODUCTION

The sisal fiber from *Agave sisalana* is the most important leaf fiber in terms of quality and commercial use.<sup>1,2</sup> The plant, which is native to Central America, has been used since pre-Columbian times. Nowadays, Brazil is the major producer, with more than a million of people depending on this crop in the northeast region of the country.<sup>3</sup>

Sisal is a hard fiber extracted from the leaves. A sisal plant produces roughly 200–250 leaves, each containing 1000–1200 fiber bundles, which consist of 4% fiber, 0.75% cuticle, 8% dry matter, and 87.25% water.<sup>4,5</sup> The extraction of fibers from the sisal plant is done through the cutting and decortication of the leaves and then the washing, drying, and cleaning of the fibers.<sup>3</sup> The fiber length ranges between 1.0 and 1.5 m, and the diameters are 100–300  $\mu\text{m}$ .<sup>1</sup> The fibers are multicellular with small individual cells, ultimate cells, bonded together.<sup>1,6</sup> These ultimate cells are the reinforcements for hemicellulose and lignin matrices. Therefore, the cell wall is a composite structure of

lignocellulosic material reinforced by helical microfibrillar bands of cellulose. This composite material is surrounded by waxy cuticle layers, which make interactions with the rubber matrix poor. Besides, cellulose is a hydrophilic glucan polymer consisting of a linear chain of 1,4- $\beta$ -bonded anhydroglucose units, and the presence of hydroxyl groups will lead to a very poor interface between the sisal fiber and the hydrophobic matrix and very poor moisture absorption resistance.<sup>1,7</sup>

In recent years, there has been increasing interest in finding new applications for sisal-fiber-reinforced composites on account of its low cost and density, high specific strength and modulus, availability in tropical countries, and renewability.<sup>2,8</sup> Although sisal is one of the most widely used natural fibers, a large quantity of it is still underused.<sup>1</sup> Sisal fibers are mainly applied to ropes for the marine and agricultural industries, cords, upholstery, padding, and mat making.<sup>1,5</sup> The use of sisal fibers as a reinforcement in composites has raised great interest and expectations among materials scientists and engineers. The quality of the fiber–matrix interface is significant for the application of sisal fibers as reinforcement fibers for polymers and rubbers. Physical and chemical methods have been used to optimize the enhancement of the fiber–polymer interface.<sup>6–10</sup> As a result, the pretreatment of the fibers results in chemical and structural changes in the fibers, which in turn influence the properties of the fibers and composites.<sup>11</sup>

Correspondence to: I. Joeques (ines@iqm.unicamp.br).

Contrast grant sponsor: Conselho Nacional de Desenvolvimento Científico e Tecnológico.

Contrast grant sponsor: Fundação de Amparo à Pesquisa do Estado de São Paulo; contract grant number: 00/14760-7.

Scanning electron microscopy (SEM) is one of the most versatile tools available for the examination and analysis of microstructural and morphological characteristics of materials, including fibers.<sup>12</sup> Many studies on the morphological properties of various natural fibers have been reported, including studies of chemical modification,<sup>13–21</sup> structural investigation,<sup>22</sup> and thermal characterization.<sup>23–25</sup> SEM has also been used to investigate the effect of surface treatments of fibers on the properties of polymers and rubber composites<sup>26–30</sup> to study the effects of processing conditions on the dimensions of sisal fibers in thermoplastic, biodegradable composites<sup>31</sup> and to investigate microstructures and fracture surfaces in composites.<sup>32</sup>

In this work, SEM was used to study the structural and morphological changes of Brazilian sisal fibers after mercerization (an alkali treatment) and acetylation. These fibers were used as reinforcements for the manufacturing of composite materials with tire rubber as the matrix, and the results showed that the chemical treatments of the fibers improved the performance of the composites.<sup>33,35</sup>

## EXPERIMENTAL

### Materials

Sisal fibers, from the variety *A. sisalana*, were supplied by Brazilian Agricultural Research Corp. (Embrapa/CNPA, Campina Grande, Brazil). The sisal-fiber samples used were from the first year of harvest (which is ready about 3 years after planting from the nursery stage) and were the waste after decortication. Decortication involves the separation of the fibers from the leaves, washing, drying, combing, and baling. The samples used in this work were the waste obtained in the last two steps. In a previous article,<sup>33</sup> we reported the average density of the fibers as  $1.26 \pm 0.03 \text{ g/cm}^3$ , measured in a helium pycnometer with 10 runs for each one of the 10 samples analyzed,<sup>36</sup> and the average diameter, measured on 100 fibers with a micrometer, as  $114 \pm 40 \text{ }\mu\text{m}$ . The average chemical composition for this variety is as follows:  $75.2 \pm 0.3\%$  cellulose,  $13.9 \pm 0.1\%$  hemicellulose,  $8.0 \pm 0.1\%$  lignin, and  $0.87 \pm 0.01\%$  ash.<sup>33,34</sup>

Analytical-grade sodium hydroxide (NaOH), sulfuric acid ( $\text{H}_2\text{SO}_4$ ), glacial acetic acid, acetic anhydride, osmium tetroxide, propylene oxide, and glutaraldehyde reagents were used. All reagents were used as received.

### Methods

#### I

Before the chemical modification, samples of raw or untreated sisal fibers were washed in distilled water at  $80 \pm 2^\circ\text{C}$  for 1 h. The washed fibers were mercerized

with 5 and 10% NaOH at room temperature ( $26 \pm 2^\circ\text{C}$ ), at 50 and  $80^\circ\text{C}$ , for 1, 3, and 5 h, rinsed with tap water, neutralized with acetic acid, and dried in a microwave oven for 15 min.<sup>33,35</sup>

#### II

Samples (50 g) of raw sisal fibers were immersed in glacial acetic acid for 1 h at room temperature ( $26 \pm 2^\circ\text{C}$ ) and then immersed in 500 mL of acetic anhydride containing 20 drops of concentrated  $\text{H}_2\text{SO}_4$  for 5 min. The fibers were separated in a Buchner funnel, rinsed with tap water at pH 6–7, and dried in a microwave oven for 15 min.<sup>33,35</sup> Mercerized fibers were acetylated with the same method.

#### III

The samples were glued onto stubs and coated with gold with a Sputter Edward S 150 B (BOC Edwards, Sussex, UK) coating apparatus. An SEM instrument (JEOL JSM 840A, Jeol Ltd., Tokyo, Japan) operating at 25 kV was used to study the structure, morphology, and fracture surface of the sisal fibers. Another set of fibers was immersed in liquid nitrogen for 15 min and was fractured. The fractured surfaces were then scanned.

#### IV

For the analysis of the transverse surfaces of the sisal fibers, 1-cm segments of raw fibers were fixed with 2.5% glutaraldehyde for 3 h at room temperature and washed with a 0.05M sodium cacodylate pH 7 buffer solution for 2 h. For postfixation, the samples were immersed in 1% (v/v)  $\text{OsO}_4$  for 1 h and then washed in distilled water and buffer. The segments were dehydrated twice with several ethanol solutions of increasing concentration (from 50 to 100% v/v) for 15 min. Also, the sisal fibers were exposed two times to a solution of ethanol and propylene oxide (1:1 v/v) for 5 min. A Spurr resin (a standard formulation with a low hardening rate and 0.2 g of catalyst) was used as an embedding medium<sup>37</sup> in the following steps: (1) sisal-fiber segments were added to closed flasks filled with Spurr and propylene oxide (1:1 v/v) solutions, (2) the flasks were placed in an acrylic rotor at a 3 rpm constant rotation for 4–8 days, (3) the flasks were opened for propylene oxide evaporation for 24 h, and (4) the fiber segments were transferred to proper inclusion molds with pure Spurr resin for 24 h and were left to cure at  $70^\circ\text{C}$  for 24 h. The transverse sections of the block obtained from the molds were cut with a Sorvall Porter–Blum MT2-B (Norwalk, CT) ultramicrotome.

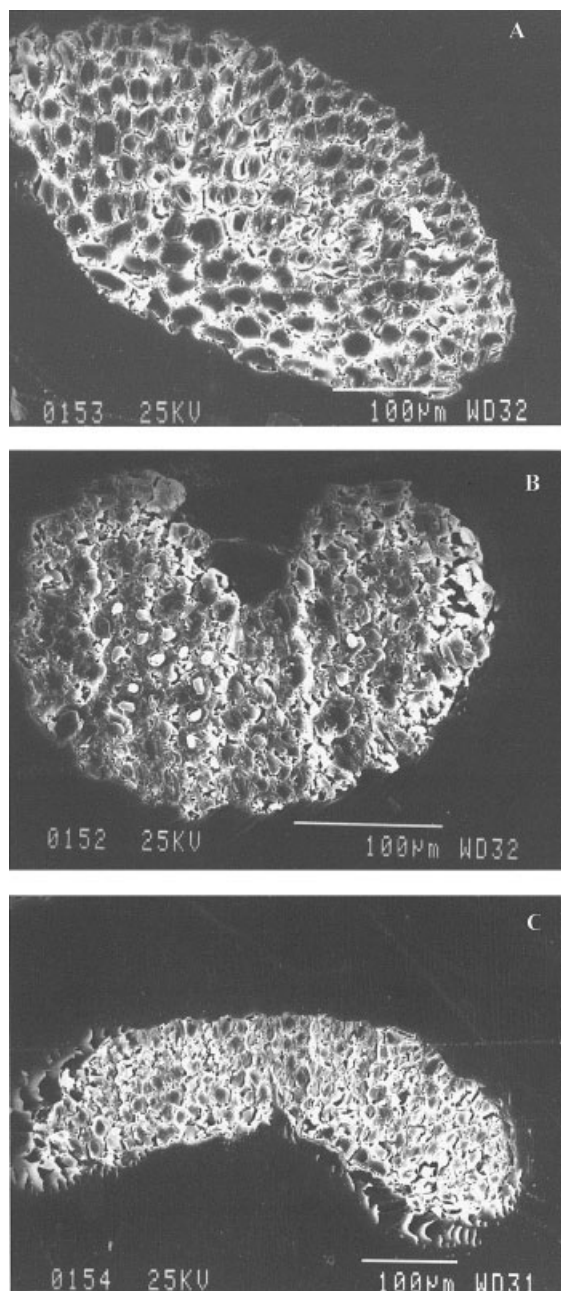


**Figure 1** SEM micrographs of the transverse sections of chemically fixed, dehydrated, and embedded untreated sisal fibers: (A) mechanical, (B) ribbon, and (C) xylem.

## RESULTS AND DISCUSSION

The sisal leaf contains three types of fibers: mechanical, ribbon, and xylem.<sup>1,4,38</sup> The mechanical fibers are mostly found around the periphery of the leaf, whereas the ribbon fibers occur in association with the conducting tissues in the median line of the leaf, and the xylem fibers occur in opposition to the ribbon fibers. To study which types of fibers our samples had, we used transversal sections of embedded fibers. The results showed that waste from decortication contained all three types. Figure 1 shows representative

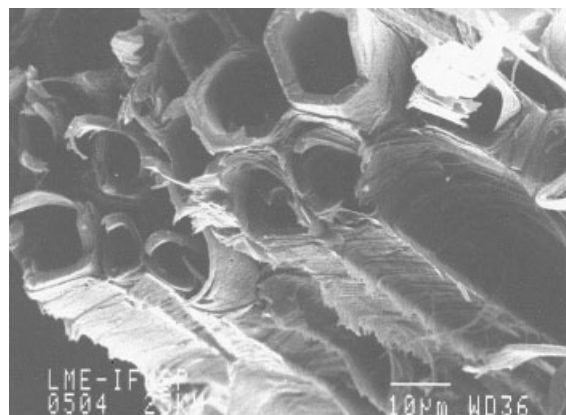
cross-sectional views. The mechanical fibers [Fig. 1(A)] are the most commercially important, but because they are seldom separated during decortication, their number is small in the waste. They are the most predominant, and their fineness dictates the grading and general commercial usefulness of sisal fibers. They are rarely circular in shape or are associated with conducting tissues. A ribbon fiber is shown in Figure 1(B); these are the longest fibers, and compared with the mechanical fibers, they easily split longitudinally. Because they occur in association with the conducting tissues, which gives them considerable mechanical strength, they have some commercial importance. Xylem fibers [Fig. 1(C)] have an irregular shape, being separated from the ribbon fibers in the vascular bundles. They are composed of thin-walled cells and therefore are easily broken and lost during the extraction processes; this makes them commercially less important.<sup>1,4,38</sup>

Transversal surface examinations were performed on cryofractured samples to evaluate the shape of the ultimate cells and the effects of the chemical treatments on the fiber bundle. Figure 2 shows representative micrographs of these cryofractured cross-sectional views of the sisal fibers. A single sisal fiber is made of several elongated fibers cells, which are also called ultimate cells. The multicellular structure of the fiber cells is characterized by a large lumen, the middle lamella (in which the lignin content is known to be concentrated), and the thickened walls. These cells are mainly polygonal in shape, as shown in Figure 2, and the lumen is rounded or has rounded corners. Extensive SEM observations of the fibers have shown that the shape of the lumen varies and is well defined, as shown in Figure 2. The shapes of these ultimate cells of sisal fibers vary considerably; they range in length from 1.5 to 4.0 mm, the average length being about 3 mm. The width varies from 10 to 30  $\mu\text{m}$ , and so each ultimate cell is many times longer than its width. Roughly, 100 ultimate cells are used to form one mechanical fiber, in the basal region of the leaf, and this number decreases toward the tip of the leaf.<sup>3</sup>

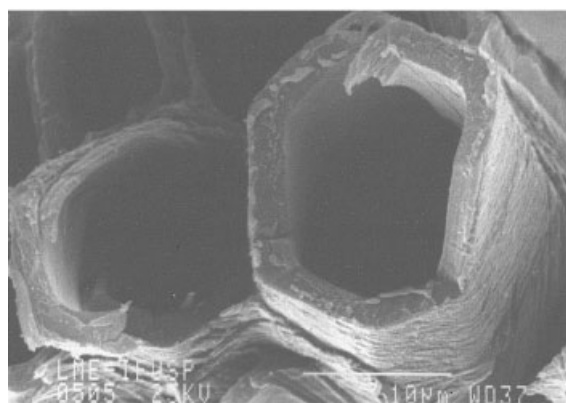
In this part of the article, we discuss the changes induced by the chemical treatments on the surfaces of the fibers because they showed improved performance as reinforcements in composite materials. The longitudinal morphology of raw or untreated sisal fibers is shown in Figure 3. The multifibrillar nature of the fiber can be observed, and the ultimate cells are arranged uniformly. The fiber surface is marked by the characteristic vestigial attachment of the parenchymatous cells in which the fiber is embedded in the leaf.<sup>15</sup>

Modifications on the surfaces of the fibers at each time, temperature, and caustic soda concentration were studied to determine the best treatment condi-

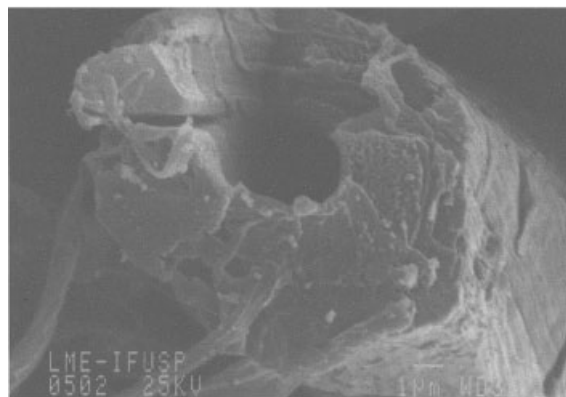




(A)



(B)



(C)

**Figure 2** SEM micrographs of the fracture surfaces of untreated sisal fibers: (A) and (B) are ultimate cells of hexagonal shape, (C) is an ultimate cell of circular shape.

tions. Figure 4 shows representative SEM micrographs of the longitudinal surface structure of fibers treated with 5% NaOH for 5 h at 50°C [Fig. 4(A)], with 10% NaOH for 1 h at room temperature [Fig. 4(B)], and with 10% NaOH for 5 h at 50°C [Fig. 4(C)]. The surfaces of the fibers significantly changed, showing the partial loss of the parenchyma cells. The removal of

the surface impurities and the separation of ultimate cells due to the extraction of the cementing components, such as lignin and hemicellulose, were observed after NaOH treatment. This increase in the separation of the ultimate cells resulted in increase in the effective surface area available for contact with any matrix. It was also observed that the fibrillar structure and the separation of the ultimate cells were greater with mercerized fibers (Fig. 4) than with untreated fibers (Fig. 3). The dissolution of waxy materials increased the interfibrillar region and yielded a surface with a rough texture. Other substances associated with the cellulose (i.e., noncellulosic, monosaccharide, fatty substances) and inorganic components were also removed.<sup>14</sup> No significant differences in the fiber morphology were observed by SEM with respect to the variation of the three parameters studied: the concentration, time, and temperature.

Usually, the effects of mercerization on the properties of natural fibers depend on the type and concentration of the alkali solution as well as the temperature and time of treatment.<sup>11</sup> It is well known that an alkali treatment dissolves and leaches out the fatty acids and their condensation products that form the waxy cuticle layer.<sup>6,7,14</sup> However, the SEM study showed that the parenchyma cells were only partially removed and that the morphological changes were independent of the treatment conditions used. Fibers submitted to less severe treatment conditions [Fig. 4(B)] showed more significant changes than those submitted to severe conditions [Fig. 4(C)]. These results were observed for all the fibers studied under all the different mercerization conditions, indicating that it was possible to use less drastic and more economical treatment conditions. Gravimetric results<sup>33,35</sup> obtained after the mercerization treatment showed that the mass loss depended more on the temperature than on the time and that mercerization led to an average mass loss of  $22 \pm 3\%$  (w/w) for 5% NaOH and  $27 \pm 5\%$  (w/w) for

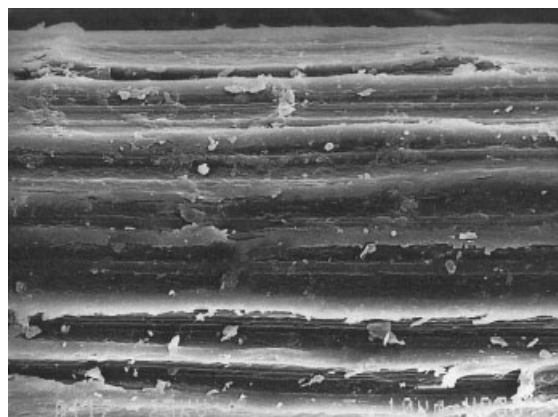
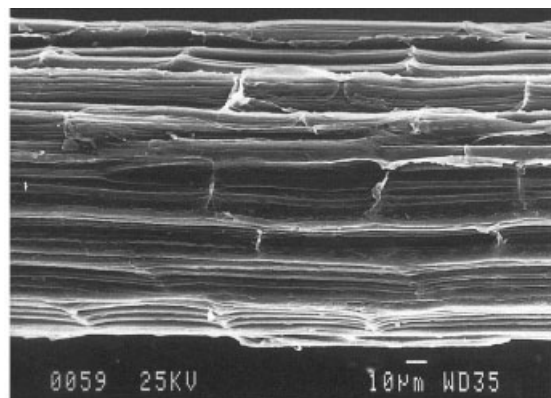
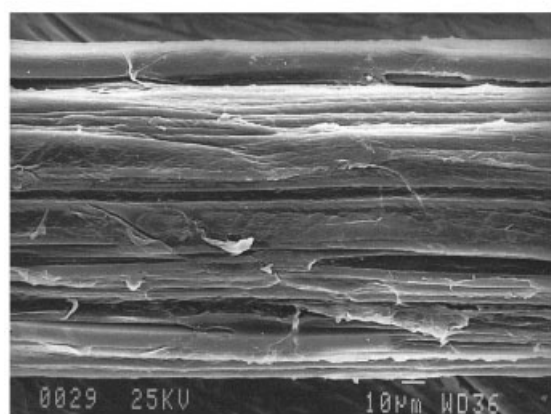


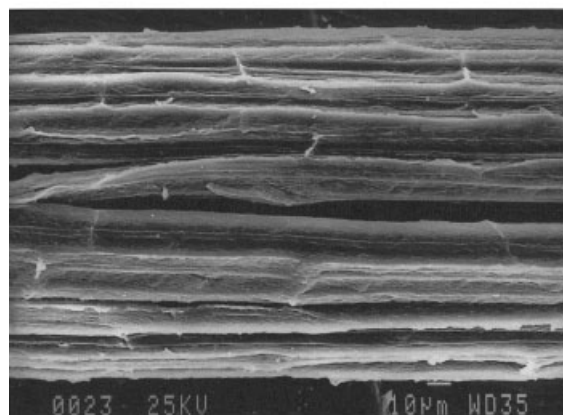
**Figure 3** SEM micrograph of the longitudinal section of an untreated sisal fiber (scale bar = 10  $\mu\text{m}$ ).



(A)



(B)



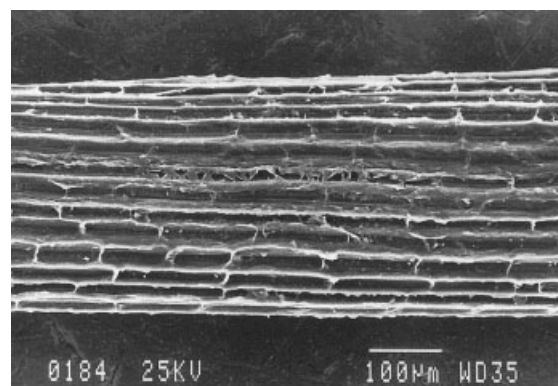
(C)

**Figure 4** SEM micrographs of the longitudinal sections of sisal fibers mercerized under different conditions: (A) 5% NaOH, 5 h, and 50°C; (B) 10% NaOH, 1 h, and room temperature; and (C) 10% NaOH, 5 h, and 50°C.

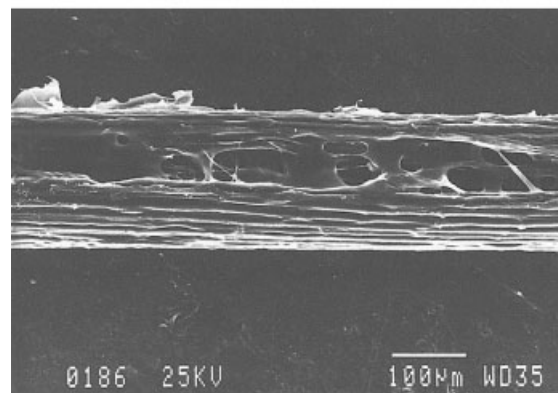
10% NaOH. Infrared and mid-infrared results showed that lignin and hemicellulose were removed from the surface and from the inner part of the bundles. The removal of soluble matter during washing contributed to the mass loss.<sup>33,35</sup>

Representative SEM micrographs of the surface structures of acetylated fibers are shown in Figure 5.

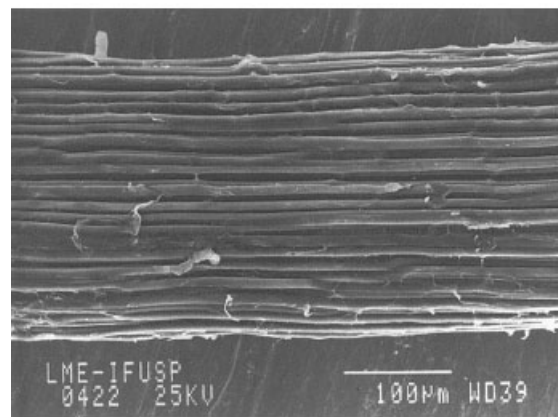
This part of the work was done to study morphological changes and the degree of acetylation of the untreated and mercerized fibers. Figure 5(A) shows an acetylated untreated fiber; most of the acetylated untreated sisal fiber exhibited the macroscopic visual aspect of the original fiber, despite the partial loss of the parenchyma cells and the presence of defibrillation at some points. Figure 5(B,C) shows mercerized (5%



(A)



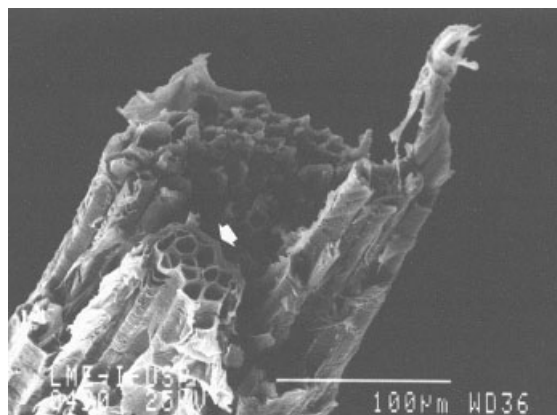
(B)



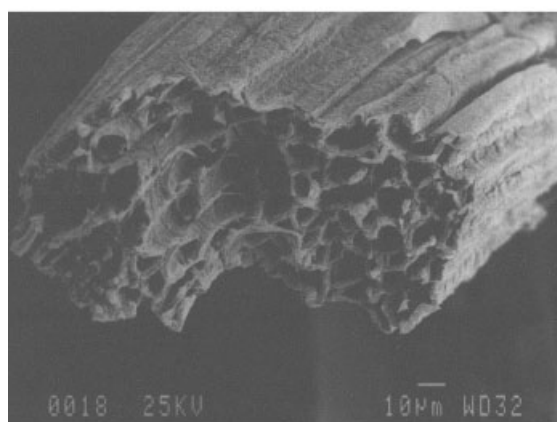
(C)

**Figure 5** SEM micrographs of (A) acetylated untreated and (B,C) mercerized (5% NaOH, 5 h, and 80°C) and acetylated sisal fibers.

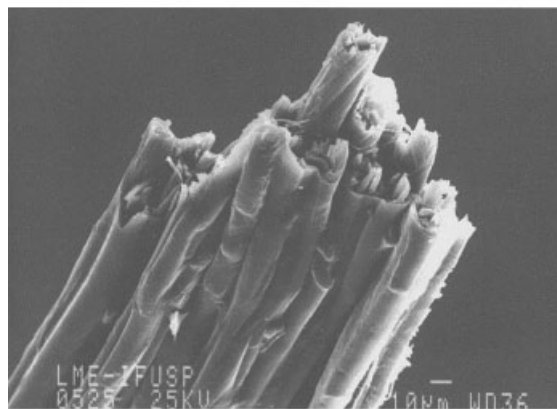




(A)



(B)



(C)

**Figure 6** SEM micrographs of the fracture surfaces of (A) untreated, (B) mercerized, and (C) mercerized and acetylated sisal fibers. The arrow shows conductive vessels.

NaOH for 5 h at 80°C) and acetylated fibers in which a coating with cellulose acetate due to the heavy incorporation of acetyl groups in the fibrils was evident, as also shown by Fourier transform infrared (FTIR).<sup>33</sup> In Figure 5(C), the fibrils are more distinct and are beginning to defibrillate.

In Figure 6, representative micrographs of the cryo-fractured surfaces of untreated and treated fibers are shown. Figure 6(A) shows the conducting vessels of the vascular bundle (e.g., the phloem and xylem in plant leaves), as indicated by an arrow, of an untreated fiber. The conducting vessels often split during decortication. Figure 6(B) shows a mercerized fiber (10% NaOH for 1 h at 80°C), indicating that the chemical treatment removed the impurities and waxy materials on the fiber surface. The fracture surface of a mercerized and acetylated fiber is shown in Figure 6(C). The fiber surface was coated with cellulose acetate because of the addition of acetyl groups. The intercellular space in the fiber was filled by lignin, which bound the fibers cells to form fiber bundles; the treatment conditions used to remove lignin and hemicellulose modified the fiber surface but did not damage the fiber structure; that is, the ultimate cells remained joined in a bundle, as also shown by FTIR and tensile tests.<sup>33</sup>

Figures 7–10 show the effects of the treatments on the conductive vessels. As the studied fibers were decortication waste, the conductive vessels were more frequently present. Figure 7(A) shows cross-sectional

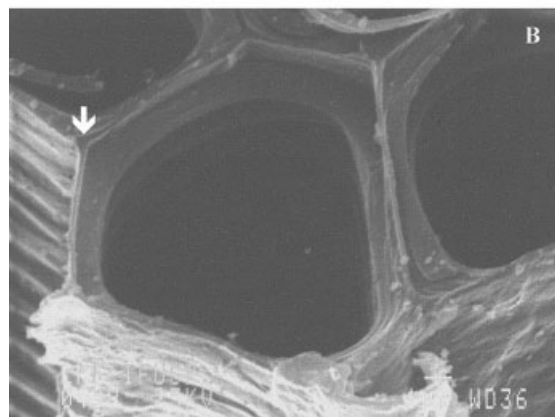
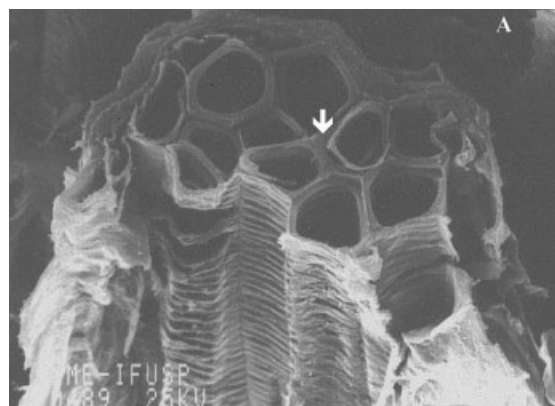


**Figure 7** (A) SEM micrograph (scale bar = 10 µm) of the conductive vessels present in untreated sisal fiber shown in Figure 6 (A). Micrograph (B) (scale bar = 1 µm) is a detail of (A). The arrows show the middle lamella.

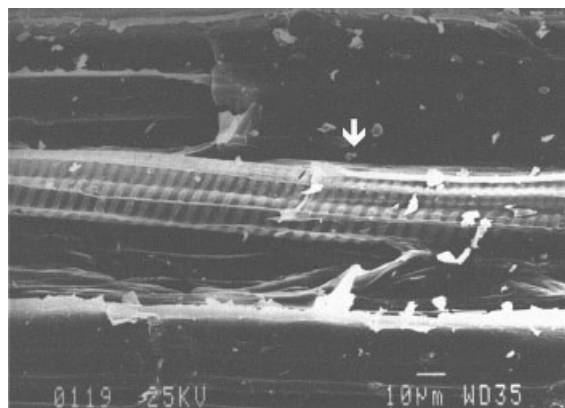


**Figure 8** SEM micrograph of the longitudinal section of an untreated sisal fiber. The arrow shows conductive vessels present in the fiber.

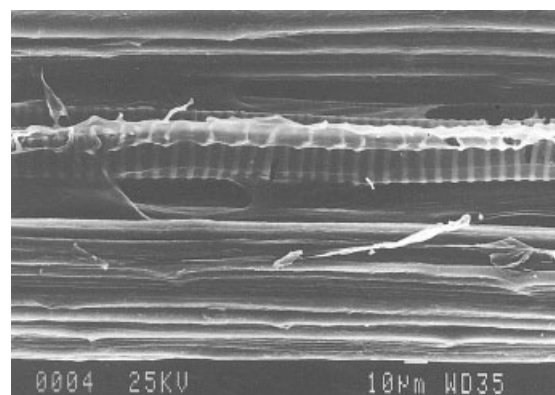
views of fibers, examined at higher magnifications, of the spirally thickened conductive vessels of Figure 6(A). These conductive vessels exhibited a large lumen and a thin continuous wall, with rings or spirals of secondary-wall material obtained inside the vessels. At higher magnifications [Fig. 7(B)], the outer layer thickness of one spiral vessel was about  $0.3 \mu\text{m}$ . The lumen was larger than the thickness of the secondary wall. The middle lamella binding the cells together could be observed between the cells, as indicated by arrows. Uncoiling these vessels was easy when the fibers were tested in tension.

Figures 8–10 show longitudinal views of sisal fibers exhibiting morphological changes in the conductive vessels after mercerization or mercerization and acetylation. Figure 8 shows a conductive vessel, indicated by an arrow, present in an untreated sisal fiber. The vessel was covered by a thin primary wall and the impurities and waxy cuticle layers. After mercerization (Fig. 9), the impurities were removed without structural damage in all cases. Depending on the treatment conditions, the single spiraled fibril of the conductive vessels could be even exposed because the primary wall was dissolved away. Some defibrillation could also be observed. Representative SEM micrographs of mercerized and acetylated fibers in which conductive vessels were present are shown in Figure 10. Both the fiber and the conductive-vessel surfaces were covered with cellulose acetate; this indicated that acetylation changed the morphology of the conductive vessels without damaging the fiber bundle.

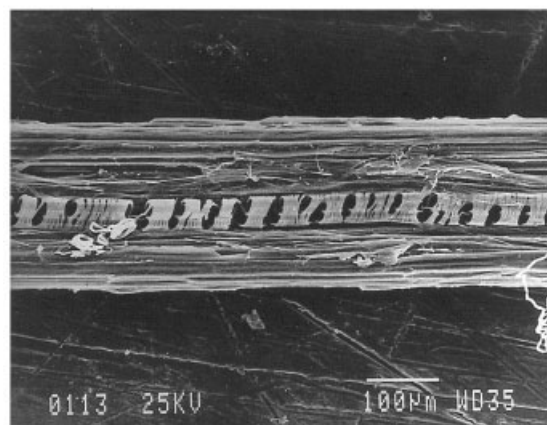
## CONCLUSIONS

In a previous work,<sup>33</sup> infrared characterization, thermogravimetric analysis, mechanical tensile properties, and water sorption data of fibers and tire-rubber composites were reported. An interesting feature of the

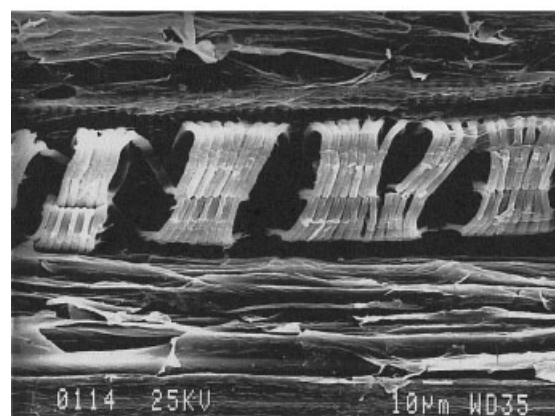
composites was that, unexpectedly, they showed properties as good as those of composites reinforced with agave mechanical fibers. Because the fibers studied in this work were waste, this opens up new applications for them. On the other hand, this work shows



(A)



(B)



(C)

**Figure 9** SEM micrographs of the conductive vessels in longitudinal sections of sisal fibers mercerized under different conditions: (A) 5% NaOH, 1 h, and room temperature and (B,C) 10% NaOH, 1 h, and room temperature. Micrograph C is a detail of micrograph B.

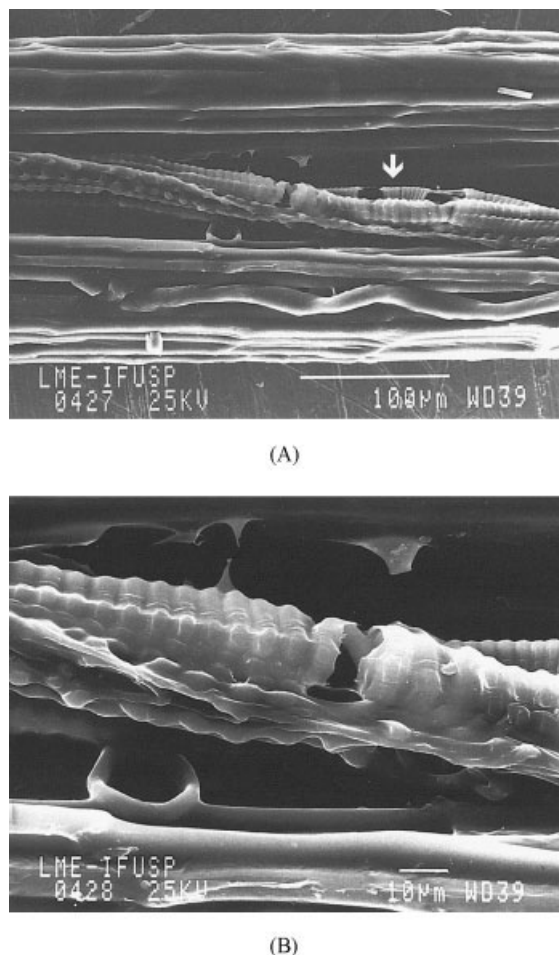


**Figure 10** (A) SEM micrograph of the longitudinal sections of mercerized and acetylated sisal fibers, showing the conductive vessels. Micrograph (B) is a detail of (A).

that the treatments used change the morphology without damaging the fiber structure, as indicated by tensile tests. Morphology changes are mainly due to an increase in the effective surface area available for adhesion to the rubber matrix, and this could account for the unexpected performance.

The authors thank Embrapa/CNPA for the sisal fibers.

## References

- Li, Y.; Mai, Y.; Ye, L. *Compos Sci Technol* 2000, 60, 2037.
- Encyclopedia of Polymer Science and Engineering; Wiley: New York, 1989; Vol. 16.
- Mattoso, L. H. C.; Ferreira, F. C.; Curvelo, A. A. S. In *Lignocellulose-Plastic Composites*; Leão, A. L.; Carvalho, F. X.; Frollini, E., Eds.; Universidade de São Paulo/Universidade Estadual Paulista: São Paulo, Brazil, 1997.
- Bisanda, E. T. N.; Ansell, M. P. *J Mater Sci* 1992, 27, 1690.
- Mukherjee, P. S.; Satyanarayana, K. G. *J Mater Sci* 1984, 19, 3925.
- Mwaikambo, L. Y.; Ansell, M. P. *Angew Makromol Chem* 1999, 272, 108.
- Bledzki, A. K.; Gassan, J. *Prog Polym Sci* 1999, 21, 221.
- Hill, C. A. S.; Khalil, H. P. S. A.; Hale, M. D. *Ind Crop Prod* 1998, 8, 53.
- Bledzki, A. K.; Reihmane, S.; Gassan, J. *J Appl Polym Sci* 1996, 59, 1329.
- Joseph, P. V.; Rabello, M. S.; Mattoso, L. H. C.; Joseph, K.; Thomas, S. *Compos Sci Technol* 2002, 62, 1357.
- Rong, M. Z.; Zhang, M. Q.; Liu, Y.; Yang, G. C.; Zeng, H. M. *Compos Sci Technol* 2001, 61, 1437.
- Hearle, J. W. S.; Simmens, S. C. *Polymer* 1973, 14, 273.
- Sreekala, M. S.; Kumaran, M. G.; Thomas, S. *J Appl Polym Sci* 1997, 66, 821.
- Mwaikambo, L. Y.; Ansell, M. P. *J Appl Polym Sci* 2002, 84, 2222.
- El-Naggar, A. M.; El-Hosamy, M. B.; Zahran, A. H.; Zohdy, M. H. *Am Dye Rep* 1992, 81, 40.
- Baiardo, M.; Frisoni, G.; Scandola, M.; Licciardello, A. *J Appl Polym Sci* 2002, 83, 38.
- Sabaa, M. W.; Mikhael, M. G.; Elkholly, S. S.; Elsabee, M. Z. M. *Cellul Chem Technol* 1995, 29, 671.
- Rout, J.; Tripathy, S. S.; Nayak, S. K.; Misra, M.; Mohanty, A. K. *J Appl Polym Sci* 2001, 79, 1169.
- Ghosh, P.; Datta, C. *J Mater Sci* 1990, 25, 4415.
- Chand, N.; Verma, S.; Khazanchi, A. C. *J Mater Sci Lett* 1989, 8, 1307.
- Barkakaty, B. C. *J Appl Polym Sci* 1979, 24, 269.
- Barkakaty, B. C. *J Appl Polym Sci* 1976, 20, 2921.
- Silva, G. G.; Souza, D. A.; Machado, J. C.; Hourston, D. J. *J Appl Polym Sci* 2000, 76, 1197.
- Chand, N.; Sood, S.; Singh, D. K.; Rohatgi, P. K. *J Therm Anal* 1987, 32, 595.
- Chand, N.; Hashmi, S. A. R. *J Mater Sci* 1993, 28, 6724.
- Vignon, M. R.; Dupeyre, D.; Garcia-Jaldon, C. *Bioresource Technol* 1996, 58, 203.
- Paul, A.; Joseph, K.; Thomas, S. *Compos Sci Technol* 1997, 57, 67.
- Flink, P.; Stenberg, B. *Br Polym J* 1989, 21, 259.
- Varghese, S.; Kuriakose, B.; Thomas, S.; Koshy, A. T. *J Adhes Sci Technol* 1994, 8, 235.
- Kumar, R. P.; Amma, M. L. G.; Thomas, S. *J Appl Polym Sci* 1995, 58, 597.
- Iannace, S.; Ali, R.; Nicolais, L. *J Appl Polym Sci* 2001, 79, 1084.
- Song, X. M.; Hwang, J. *Wood Fiber Sci* 1997, 29, 131.
- Martins, M. A.; Joekes, I. *J Appl Polym Sci* 2003, 89, 2507.
- Martin, A. R. Ph.D. Thesis, Universidade Federal de São Carlos, 2001.
- Martins, M. A. Ph.D. Thesis, Universidade Estadual de Campinas, 2001.
- Mwaikambo, L. Y.; Ansell, M. P. *J Mater Sci Lett* 2001, 20, 2095.
- Spurr, A. R. *J Ultrastruct Res* 1969, 26, 31.
- Nutman, F. J. *Empire J Exp Agr* 1936, 5, 75.